Efficient Electromagnetic Modeling of Microstrip Structures in Multilayer Media

Feng Ling, *Student Member, IEEE*, Dan Jiao, and Jian-Ming Jin, *Senior Member, IEEE*

***Abstract*—This paper presents an efficient method-of-moments solution of the mixed-potential integral equation for a general microstrip structure in multilayer media. In this method, the general forms of the spectral-domain Green's functions for multilayer media are derived first. The spatial-domain Green's functions are then obtained by the discrete complex-image method, which obviates the time-consuming numerical evaluation of the Sommerfeld integral. The Rao–Wilton–Glisson basis functions are employed to provide necessary flexibility to model arbitrary shapes. To expedite the computation of frequency response over a broad band, a reduced-order model is presented using asymptotic waveform evaluation. Numerical results of multilayer circuits and antennas are presented to show the efficiency and accuracy of this method.**

***Index Terms*— Complex-image method, Green's function, method of moments, multilayer media, reduced-order model.**

I. Introduction

A VARIETY of methods have been developed for electromagnetic modeling of microstrip structures, such as antennas, circuits, and interconnects [1]. A review of them reveals that the method-of-moments (MoM) solution of the integral equation has received intense attention. In this method, the evaluation of Green's functions and the choice of basis functions are crucial to obtaining an accurate and efficient solution. Therefore, many variations of this method have been implemented and investigated. Among them, the solution based on the mixed-potential integral equation (MPIE) using the Rao–Wilton–Glisson (RWG) basis functions [2] is an attractive approach [3]–[6] because the RWG basis function offers good flexibility to model arbitrarily shaped structures, and MPIE provides a less singular kernel compared with the electrical-field integral equation (EFIE).

On the other hand, when microstrip structures become more complicated, multilayer media are employed to allow for more versatile designs [6]–[9]. This fact necessitates the modeling to be capable of dealing with microstrip structures in multilayer media. To achieve this goal, the evaluation of Green's functions for multilayer media is crucial. As is well known, the spatial-domain Green's function is the inverse Hankel transform of the spectral-domain counterpart, which is commonly known as the Sommerfeld integral (SI). Generally, the analytical solution of the SI is not available, and the numerical integration is time consuming since the integrand is both highly oscillating and slowly decaying. Several efficient techniques have been proposed to speed up this numerical integration [10], [11]. To further accelerate the computation, the scheme that employs the precomputation and interpolation techniques is popularly used [6], [12]. Another approach to rapidly evaluate the SI is the discrete complex-image method (DCIM) [13]–[17]. The basic idea of the DCIM is to approximate the spectral kernel by a sum of complex exponentials using the Prony method or the generalized pencil-of-function (GPOF) method [18]. The SI's can then be evaluated in closed forms via the Sommerfeld identity. This method has been extensively employed to analyze microstrip structures. However, most of the work is confined to single- or double-layered structures. As claimed in [6] and [20], it is difficult to extend the DCIM to multilayer media because of the difficulty associated with the extraction of the surface-wave contribution. However, since the surface-wave contribution is insignificant for the thin multilayer configurations and becomes appreciable only in the far-field region, it is not necessary to extract the surface wave for those cases [17], thereby rendering the DCIM possible and efficient for multilayer media. In this paper, we show that the DCIM is accurate for all the examples considered without the extraction of surface-wave contribution.

Furthermore, since the above analysis is implemented in the frequency domain, we have to repeat the calculation at each frequency to obtain the frequency response over a band of interest. This can be computationally intensive for electromagnetic devices with complicated frequency responses. For this reason, several different techniques have been proposed to characterize such devices by using the reduced-order model, such as the asymptotic waveform evaluation (AWE) [22], complex frequency hopping (CFH) [23], and Padé via Lanczos (PVL) [24]. All of them were originally developed in the circuit community. The basic idea of these techniques is to approximate the frequency response or the transfer function by a low-order rational function: the Padé approximant. In AWE and CFH, the Padé approximant of the frequency response is obtained by the moment-matching process. In PVL, the Padé approximant is obtained by the Lanczos process so that the direct calculation of moments is eluded. Recently, these techniques have been extended for electromagnetic analysis [25]–[28]. A parallel effort ongoing in the electromagnetic community is the development of the model-based parameter estimation (MBPE) [29], [30]. Instead of matching moments in

Manuscript received January 15, 1999; revised May 10, 1999. This work was supported by the Air Force Office of Scientific Research Multidisciplinary Research Initiative Program under Contract F49620-96-1-0025, and by the National Science Foundation under Grant NSF ECE 94-57735.

The authors are with the Center for Computational Electromagnetics, Department of Electrical and Computer Engineering, University of Illinois at Urbana-Champaign, Urbana, IL 61801-2991 USA.

Publisher Item Identifier S 0018-9480(99)07159-8.

AWE, MBPE matches the derivatives of the transfer function to find the Padé approximant.

Although PVL is more stable than AWE, the algorithm requires the submatrices to be frequency independent. This is not the case in MoM since the submatrices are frequency dependent through the Green's functions. Therefore, the AWE is employed in this paper to achieve the fast frequency sweep. The unknown current is first expanded as a Taylor series at the expansion point. The Taylor series coefficients, or the moments, are associated with the frequency derivatives of the impedance matrix, which can be derived because of the use of the DCIM. The Padé approximant is then obtained by matching the moments. The response over a frequency band near the expansion point can be easily obtained. To obtain the broadband response, more expansion points are required. A simple binary search algorithm, as proposed in [25], is employed to automatically determine the expansion points to obtain the accurate solution over the entire broad band.

This paper begins with the MPIE formulation for a general microstrip structure in multilayer media and the MoM solution to this equation. The spectral-domain Green's functions for multilayer media is then derived. The DCIM is employed to efficiently evaluate the SI's, resulting in closed-form spatial-domain Green's functions. Combination of the Green's functions and the RWG basis functions offers an accurate and efficient MoM solution. The AWE technique is then applied to expedite the computation of frequency response over a bandwidth. Finally, numerical results are presented to demonstrate the accuracy and efficiency of this method.

II. Formulations

Consider a general multilayer medium, as shown in Fig. 1. For layer i, the permittivity and permeability are denoted as ϵ_i and μ_i, respectively. In most cases, the bottom is backed by a ground plane and the top is open. The medium is assumed to be laterally infinite. In this section, the MPIE formulation for general microstrip structures is derived. To obtain the spatial-domain Green's functions, we first analytically derive the Green's functions in the spectral domain. We then employ the DCIM to convert the spectral-domain Green's functions into the spatial domain, which can be written in closed forms. Finally, the AWE formulation is presented to expedite the calculation of frequency responses.

A. MPIE Formulation

The microstrip structures are assumed to be of infinitesimal conductor thickness and located in the ρ-plane. The induced current on the microstrips can be obtained from the MoM solution of the pertinent MPIE. We first divide the microstrips into triangular elements and then expand the current on the microstrips using the RWG basis functions. Applying Galerkin's method results in the matrix equation

$$\overline{\boldsymbol{Z}} \cdot \boldsymbol{I} = \boldsymbol{V} \tag{1}$$

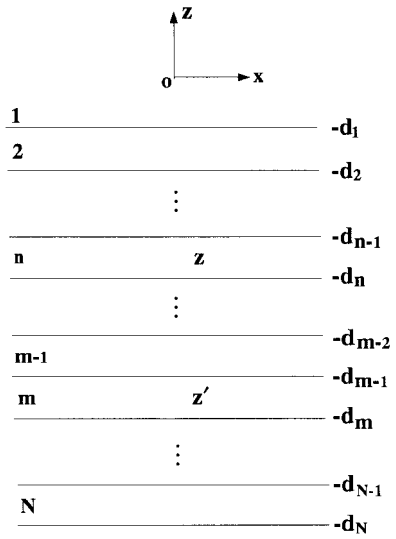

Fig. 1. A multilayer medium with source and field points in layers m and n, respectively.

in which the impedance matrix $\overline{\boldsymbol{Z}}$ and vector $\boldsymbol{V}$ have the elements given by

$$\overline{\boldsymbol{Z}}_{mn} = j\omega \iint_{Tm} \iint_{Tn} \left[\boldsymbol{f}_m(\boldsymbol{r}) \cdot \boldsymbol{f}_n(\boldsymbol{r}') G_a(\boldsymbol{r}, \boldsymbol{r}') - \frac{1}{\omega^2} \nabla \cdot \boldsymbol{f}_m(\boldsymbol{r}) \nabla' \cdot \boldsymbol{f}_n(\boldsymbol{r}') G_q(\boldsymbol{r}, \boldsymbol{r}')\right] d\boldsymbol{r}' \, d\boldsymbol{r} \tag{2}$$

$$\boldsymbol{V}_m = \iint_{T_m} \boldsymbol{E}^a(\boldsymbol{r}) \cdot \boldsymbol{f}_m(\boldsymbol{r}) \, d\boldsymbol{r} \tag{3}$$

where $\boldsymbol{f}_m$ and $\boldsymbol{f}_n$ denote the testing and basis functions, respectively, G_a is the xx-component of the Green's function for the vector potential, and G_q is the Green's function for the scalar potential. In our problems, the delta voltage source is applied at the excitation port so that the right-hand-side vector $\boldsymbol{V}$ is zero everywhere, except at the excitation edges. The current distribution on the microstrip surfaces is then obtained by solving the matrix equation (1). The S-parameters can be extracted by carefully examining the standing-wave behavior of the currents at each port.

To efficiently generate the impedance matrix $\overline{\boldsymbol{Z}}$, the fast evaluation of $G_{a,q}$ is crucial. However, the spatial-domain Green's function is represented by the SI

$$G_{a,q}(\boldsymbol{r}, \boldsymbol{r}') = \frac{1}{4\pi} \int_{-\infty}^{\infty} \tilde{G}_{a,q}(k_\rho, z, z') H_0^{(2)}(k_\rho |\boldsymbol{\rho} - \boldsymbol{\rho}'|) k_\rho dk_\rho \tag{4}$$

where $\tilde{G}_{a,q}(k_\rho, z, z')$ is the spectral-domain counterpart of $G_{a,q}(\boldsymbol{r}, \boldsymbol{r}')$. In the Section II-B, we give the general form of spectral-domain Green's functions and the efficient evaluation of the SI's by the DCIM.

B. Spectral-Domain Green's Functions

The basic principle to derive the spectral-domain Green's functions due to an arbitrary source embedded in a multilayer medium is to first decompose the fields into TE and TM waves. Their propagations in multilayer media can be characterized

by the reflection and transmission coefficients. One approach to simplify the derivations is to employ a transmission-line network analog of the multilayer medium, in which each layer is represented by a transmission-line section and the TE and TM waves are represented by two independent transmission lines [20], [21]. In this paper, the approach described in [19] is employed. For planar microstrip configurations, we consider a horizontal electric dipole (HED) embedded in layer m. The field point is located in layer n. The spectral-domain Green's functions for scalar and vector potentials can be written as

$$\tilde{G}_a = \frac{\mu_m}{2jk_{mz}} F_n^{\mathrm{TE}} \tag{5}$$

$$\tilde{G}_q = \frac{1}{2j\epsilon_n k_{mz} k_\rho^2} \left(\frac{\mu_m k_n^2}{\mu_n} F_n^{\mathrm{TE}} - jk_{mz} \frac{\partial}{\partial z} F_n^{\mathrm{TM}} \right) \tag{6}$$

where F_n^{TE} and F_n^{TM} are the TE and TM components in layer n, respectively, which can be derived as in [19].

C. DCIM

Once the spectral-domain Green's functions are obtained, the next step is to evaluate the SI, which is very time consuming because of the highly oscillating and slowly decaying behavior of the integrand. Although some techniques have been proposed for fast evaluation of the SI, the numerical integration is still the bottleneck for the design of a fast algorithm. The DCIM obviates numerical integration and represents the SI in a closed form. Initially, the DCIM first extracts the quasi-static and surface-wave contributions from the spectral-domain kernel, then approximates the remaining kernel by a sum of complex exponentials, and finally evaluates the integral via the Sommerfeld identity. Since the extraction of the surface-wave contributions for multilayer media is cumbersome, it is difficult to extend the DCIM to multilayer media. Recently, the GPOF method has been applied to cast the Green's functions into closed forms, which is more robust and less noise sensitive compared to the original Prony method. The use of GPOF also shows that the extraction of the surface-wave contributions is not necessary for structures with insignificant surface waves. This makes it easy to employ the DCIM for multilayer media.

To apply the DCIM, we rewrite the spectral-domain Green's function in a simple form as

$$\tilde{G} = \frac{F}{2jk_{mz}}. \tag{7}$$

As the first step of the DCIM, the quasi-static contributions, which dominate as $k_\rho \to \infty$, are extracted, which makes the remaining kernel decay to zero for sufficiently large k_ρ. For the TE case, the reflection coefficients approach $(\mu_i - \mu_{i+1})/(\mu_i + \mu_{i+1})$ while, in the TM case, they tend to $(\epsilon_i - \epsilon_{i+1})/(\epsilon_i + \epsilon_{i+1})$. Therefore, we can rewrite (7) as

$$\tilde{G} = \frac{F - F_0}{2jk_{mz}} + \frac{F_0}{2jk_{mz}} \tag{8}$$

where F_0 denotes the quasi-static term. With the aid of the Sommerfeld identity, the quasi-static contribution from the second term in (8) can be evaluated as

$$G_0 = F_0 \frac{e^{-jk_m\rho}}{4\pi\rho}. \tag{9}$$

The first term in (8) can be approximated as a sum of complex exponentials using the GPOF method. The deformed integration path in the complex k_{mz} is chosen as $k_{mz} = k_m[(1 - t/T_0) - jt]$, where T_0 is determined such that $F - F_0$ becomes negligible beyond T_0. Uniformly sampling $F - F_0$ on $t \in [0, T_0]$ and applying the GPOF method, we can approximate $F - F_0$ as

$$F - F_0 = \sum_{i=1}^{N_c} a_i e^{-k_{mz} b_i}. \tag{10}$$

Again using the Sommerfeld identity, we obtain

$$G = F_0 \frac{e^{-jk_m\rho}}{4\pi\rho} + \sum_{i=1}^{N_c} a_i \frac{e^{-jk_m r_i}}{4\pi r_i} \tag{11}$$

where $r_i = \sqrt{\rho^2 - b_i^2}$ is complex, which is the location of the complex image, and N_c is the number of complex images.

As mentioned in [15], when the source is in the bounded region of multilayer media, a modification of the DCIM is necessary. In that case, the exponentials are written in terms of the propagation coefficient of the unbounded layer instead of that of the source layer.

D. AWE Implementation

The solution can be achieved by solving (1). Given a frequency band, we have to repeat the solution of (1) at a set of frequencies to obtain the frequency response. For structures with a highly oscillatory frequency response, this process is computationally expensive. Several techniques to realize the fast frequency sweep have been developed, such as MBPE, AWE, CFH, and PVL. The basic principle of these techniques is to extract the dominant poles and residues of the frequency response and represent it by a reduced-order model, which is accomplished by constructing the Padé approximant of the frequency response.

In AWE, the solution of (1) can be expanded as a Taylor series at a given frequency point ω_0

$$\boldsymbol{I}(\omega_0 + \sigma) = \sum_{n=0}^{\infty} \boldsymbol{M}_n \sigma^n \tag{12}$$

where $\boldsymbol{M}_n$ is the nth moment vector and is given by

$$\boldsymbol{M}_n = \frac{1}{n!} \frac{\partial^n}{\partial \omega^n} [\overline{\boldsymbol{Z}}^{-1}(\omega) \boldsymbol{V}] \Big|_{\omega=\omega_0}. \tag{13}$$

The moments can be evaluated by the recursive relation

$$\overline{\boldsymbol{Z}}(\omega_0) \boldsymbol{M}_n = -\sum_{r=1}^{n} \frac{1}{r!} \frac{\partial^r}{\partial \omega^r} \overline{\boldsymbol{Z}}(\omega) \Big|_{\omega=\omega_0} \boldsymbol{M}_{n-r} \tag{14}$$

with the initial vector

$$\boldsymbol{M}_0 = \overline{\boldsymbol{Z}}^{-1}(\omega_0) \boldsymbol{V}. \tag{15}$$

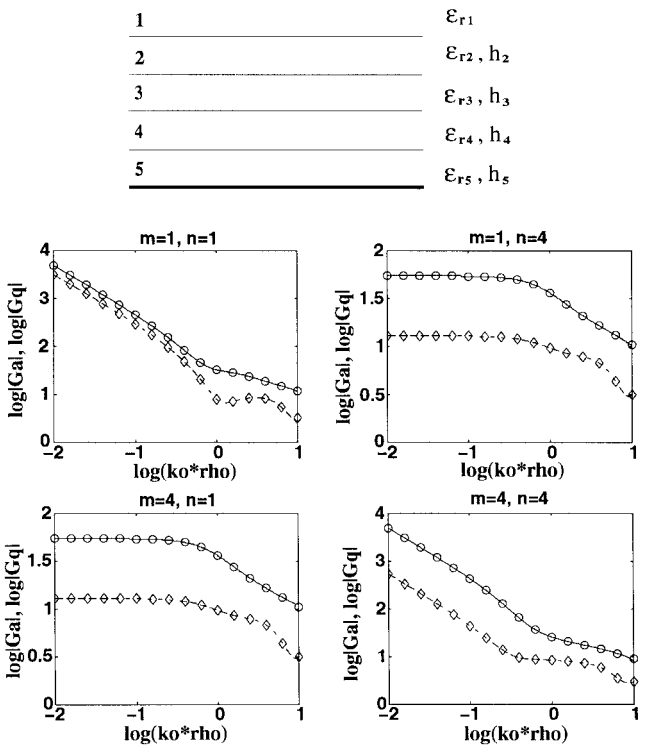

Fig. 2. Green's functions of the scalar and vector potentials in five-layer medium. The relative permittivity and thickness of each layer are as follows: $\epsilon_{r1} = 1.0$, $\epsilon_{r2} = 2.1$, $h_2 = 0.7$ mm, $\epsilon_{r3} = 12.5$, $h_3 = 0.3$ mm, $\epsilon_{r4} = 9.8$, $h_4 = 0.5$ mm, $\epsilon_{r5} = 8.6$, $h_5 = 0.3$ mm. The solid and dashed lines represent G_a and G_q, respectively, which are calculated by DCIM. The circle and diamond represent G_a and G_q, respectively, which are obtained by direct numerical integration. The frequency is 30 GHz.

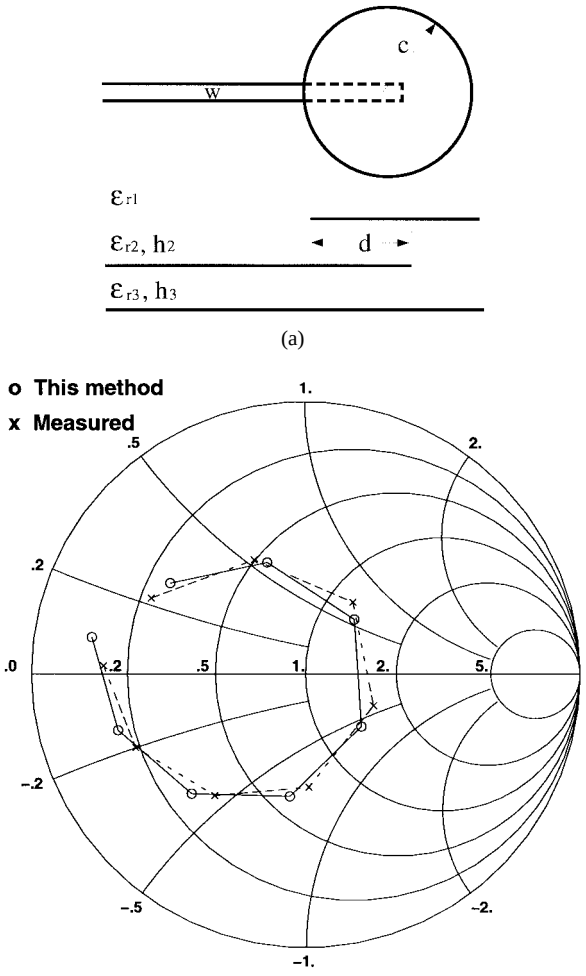

Fig. 3. Input impedance for a proximity-coupled microstrip antenna. $\epsilon_{r1} = 1.0$, $\epsilon_{r2} = \epsilon_{r3} = 2.62$, $h_2 = h_3 = 1.59$ mm, $w = 4.372$ mm, $c = 17.5$ mm, $d = 17.5$ mm. The frequency is from 2.80 to 3.15 GHz with an increment of 0.05 GHz.

To overcome the problem associated with the radius of convergence of the Taylor series expansion, the Padé approximant of $\boldsymbol{I}(\omega_0 + \sigma)$ is used, which can be written as

$$\boldsymbol{I}(\omega_0 + \sigma) = \frac{\boldsymbol{a}_0 + \boldsymbol{a}_1\sigma + \cdots + \boldsymbol{a}_p\sigma^p}{1 + \boldsymbol{b}_1\sigma + \cdots + \boldsymbol{b}_q\sigma^q} \tag{16}$$

where typically $p = q-1$ and the $p+q+1$ unknown coefficients of the numerator and denominator are uniquely determined by matching the first $p+q+1$ moments of (12), as is done in [25] and [26]. Once we obtain the Padé approximant, the frequency response over a frequency band can be rapidly evaluated.

Therefore, the first step of AWE is to evaluate the derivative matrices at the expansion point. As can be seen from (2), the impedance matrix is the function of frequency through the Green's functions. Unlike in [30], the Green's functions in this method have the simple expression e^{-jkr}/r, as is evident in (11), due to the use of the DCIM. Therefore, here, the derivative matrices can be simply formulated. The moment vectors can then be obtained recursively by (14). After the moment-matching process, the Padé approximant for each element can be obtained. Therefore, the frequency response over a band near the expansion point is obtained.

In many practical problems with a broad-band response, one expansion point is not sufficient to cover the entire bandwidth. In such cases, multiple expansion points are necessary. Here, a simple binary search algorithm, as described in [25] and [26], is employed to automatically choose the expansion points. Assume that we are interested in the frequency response over the band $[f_{\min}, f_{\max}]$. We first compute the reduced-order models using $f_{\min}$ and $f_{\max}$ as the expansion points. We then compute the frequency response over the entire band $[f_{\min}, f_{\max}]$. If the two responses are within an acceptable error tolerance, the procedure has converged. If not, an additional reduced-order model is then computed at a new expansion point $(f_{\min} + f_{\max})/2$, and the error checking process is repeated in the two new subintervals. This process is repeated until the two reduced-order models bordering all subintervals give the frequency responses within the prescribed error tolerance.

It is known that AWE has the problem of instability in the computation of the Padé approximation due to the ill-conditioned moment-matching process [24]. However, this is not a problem in our method because the order of the Padé approximant is typically chosen as $q \leq 8$, for which the instability has never been observed.

III. Numerical Results

We first verify the spatial-domain Green's functions obtained by the DCIM by considering a five-layer medium. The

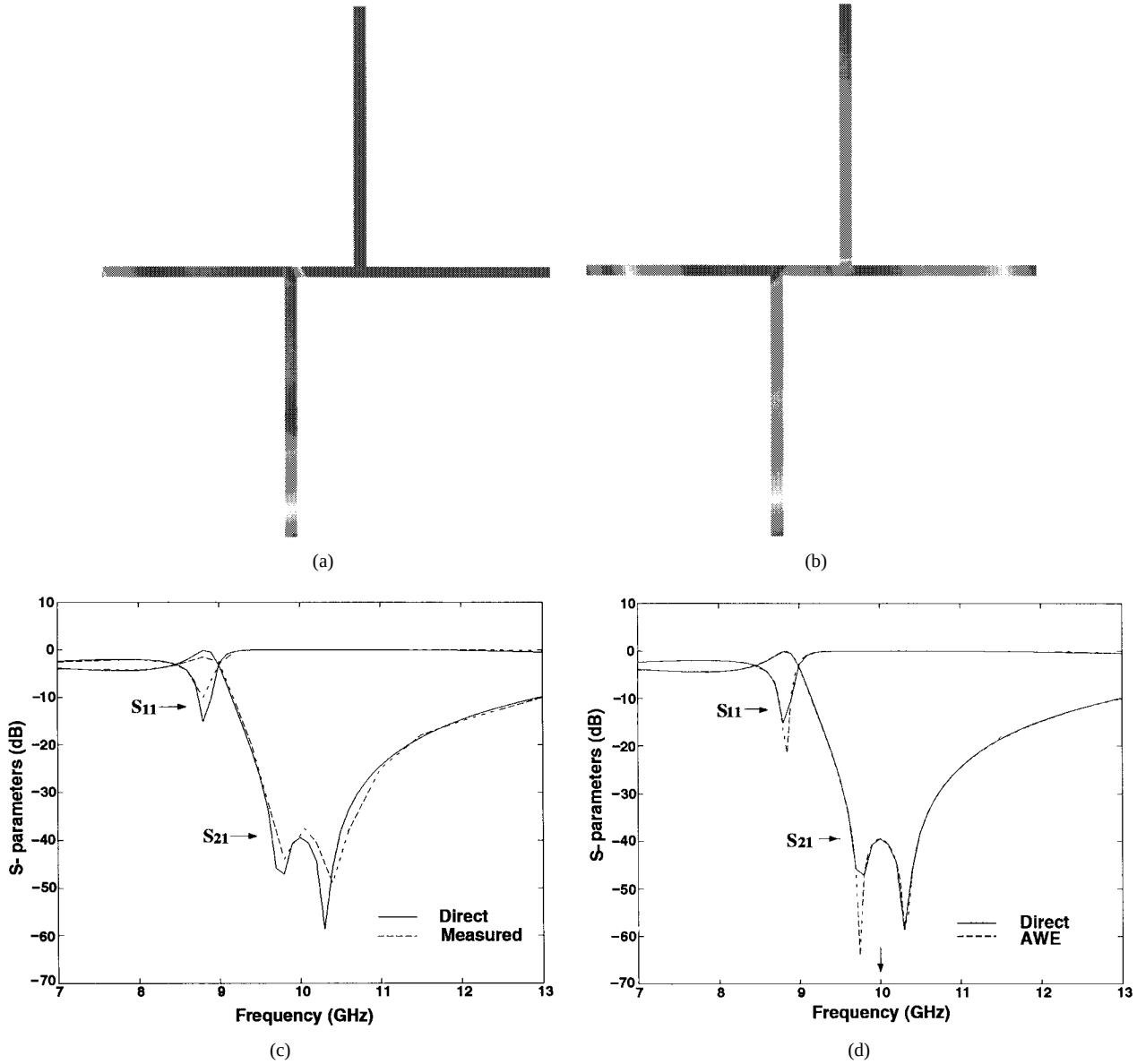

Fig. 4. Current distributions and S-parameters for a microstrip double stub. $\epsilon_r = 9.9$, $h = 0.127$ mm. The linewidth is 0.122 mm. The stub length is 2.921 mm. The spacing between two stubs is 0.757 mm. (a) $f = 10$ GHz. (b) $f = 13$ GHz.

TABLE I
COMPARISON OF THE CPU TIME USING THE DIRECT CALCULATION AND AWE

	Direct			AWE			Speed-up
	T_{freq} (sec)	N_{freq}	T_1 (sec)	T_{expn} (sec)	N_{expn}	T_2 (sec)	
Ex. 1	6.4	60	384.0	18.1	1	18.1	21.2
Ex. 2	104.0	80	8320.0	350.2	3	1050.6	7.9
Ex. 3	27.0	400	10800.0	95.9	9	863.1	12.5

T_{freq}: CPU time per frequency in the direct calculation;
N_{freq}: Number of frequencies in the direct calculation;
T_1: Total CPU time by the direct calculation;
T_{expn}: CPU time per expansion point with AWE;
N_{expn}: Number of expansion points with AWE;
T_2: Total CPU time with AWE.

first layer is free space. The fifth layer is backed by a ground plane. The frequency is 30 GHz. We seek Green's functions for the four cases. The HED can be at the interface of the first and second layer $m = 1$ or the fourth and fifth layer $m = 4$. The field point also has two choices of $n = 1$ or $n = 4$. The Green's functions of all these four cases are given in Fig. 2 compared to those obtained by the numerical integration along the Sommerfeld integration path (SIP). A good agreement can be observed. In this calculation, we choose $T_0 = 20$ and $N_c = 5$. The saving of the computation time is very significant. For instance, the average central processing unit (CPU) time to obtain one Green's function is 15 s using the numerical integration approach. In contrast, the DCIM only takes less than 0.2 s. The computation is performed on a 266-MHz DEC Alpha workstation. Furthermore, the numerical integration is performed from point to point; however, the DCIM is a plane-to-plane calculation so that the source and field points on the same z-plane share the same DCI's, which further enhances the efficiency of the DCIM.

After the validation of this technique, we incorporate the DCIM into the MoM solution of MPIE for microstrip structures in multilayer media. The example we consider is a

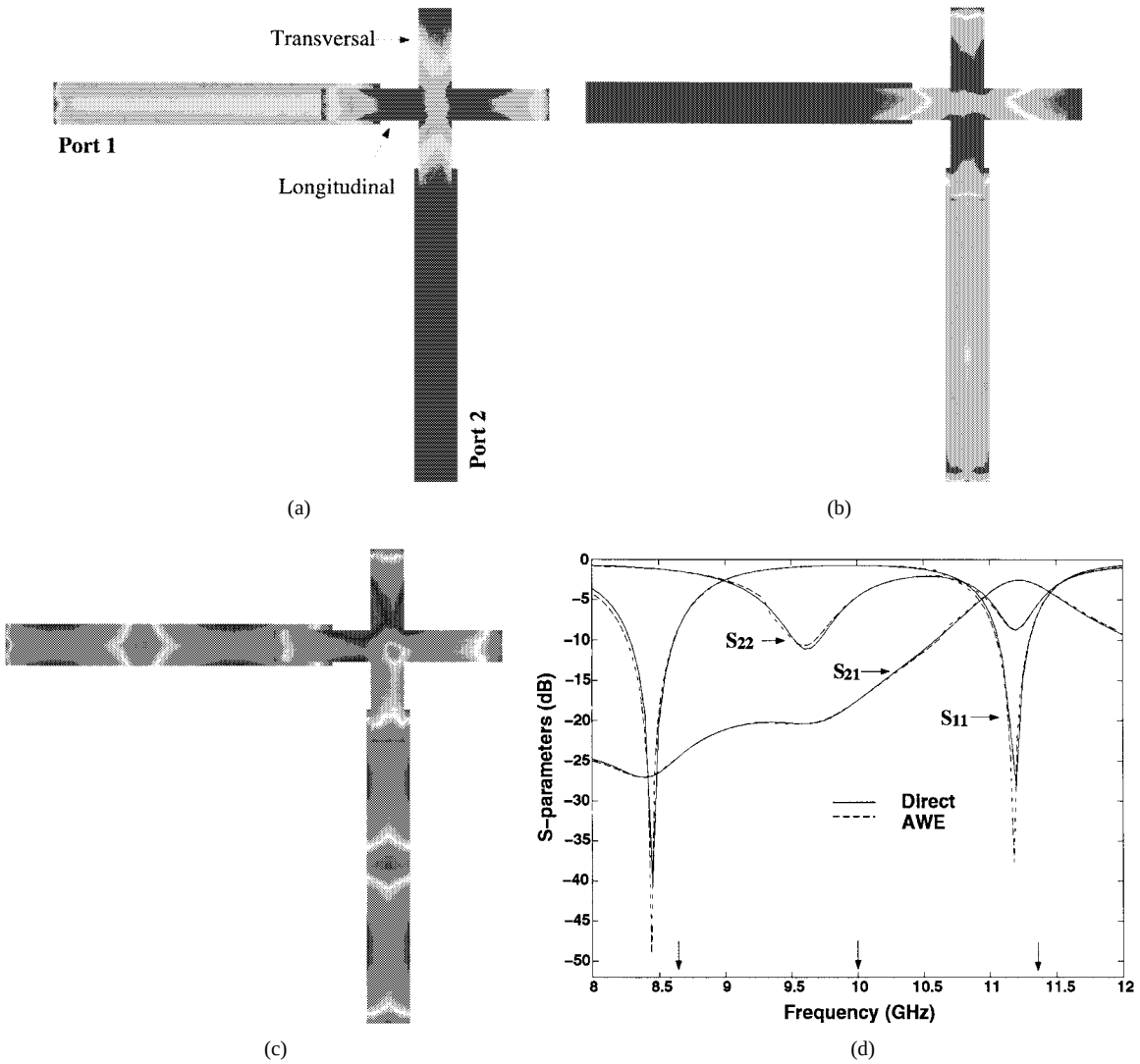

Fig. 5. Current distributions and S-parameters for a two-port asymmetric antenna. (a) $f = 8.4$ GHz. (b) $f = 9.6$ GHz. (c) $f = 11.3$ GHz.

proximity-coupled circular patch antenna [31]. The two substrate layers have the same relative permittivity $\epsilon_r = 2.62$ and thickness 1.59 mm. The microstrip line is on the bottom layer and the patch is on the top layer. The radius of the patch is 17.5 mm and the width of the microstrip line is 4.372 mm. The overlapping length may be used to control the coupling. Here, it is 17.5 mm. The number of unknowns is 686. The CPU time for one frequency is 89.3 s. The input impedance with the reference plane 79.0 mm away from the patch center is given in Fig. 3, which agrees well with the measured data from [31].

In the following three examples, AWE is applied to expedite the calculation of frequency response over a bandwidth. In all the cases, we use $q = 8$. The CPU time using AWE is compared with that employing the direct calculation to demonstrate the efficiency, as shown in Table I. We first consider a microstrip double-stub on a single layer, which has the relative permittivity $\epsilon_r = 9.9$ and the thickness 0.127 mm [12], [32]. The number of unknowns is 205. Current distributions at two different frequencies are shown in Fig. 4(a) and (b). The direct calculation gives a very good result comparing with the measured data [12], [32], as shown in Fig. 4(c). In this calculation, the CPU time at each frequency is 6.4 s and totally 60 frequencies are sampled to obtain the accurate results. Therefore, the total CPU time is 384 s. Using AWE and choosing only one expansion point $f = 10.0$ GHz, we can obtain a very good result, as given by Fig. 4(d). In the calculation with AWE, the CPU time is 18.1 s. Thus, using AWE is approximately 21 times faster. Note that the sampling points are not dense enough to catch the null at approximately 9.75 GHz for the direct calculation.

We now consider a two-port asymmetric antenna [33]. There are two orthogonally crossed dipoles on the top layer. They have different lengths so that dual-frequency operation is achieved. The transversal one has a length of 11.9 mm and the longitudinal one has a length of 10.2 mm. The width of both is 1.7 mm. The two substrate layers have the same relative permittivity $\epsilon_r = 2.17$. The top layer has a thickness of 1.6 mm and the bottom layer has a thickness of 0.8 mm. On the bottom layer, the feeding lines are 2.2-mm wide. Fed from port 1, the longitudinal dipole is excited at the resonant frequency of 8.4 GHz. The current distribution is given in

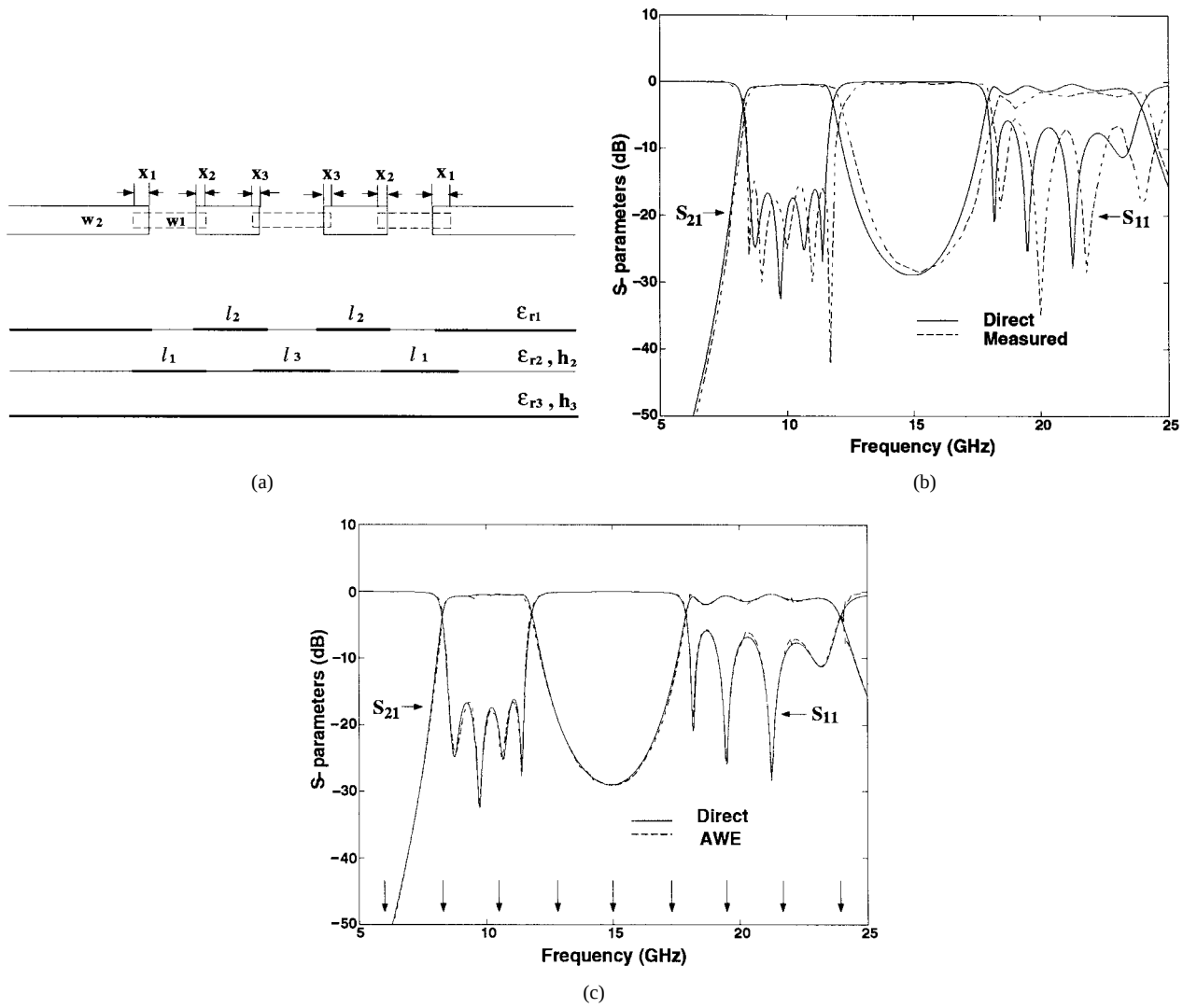

Fig. 6. S-parameters for an overlap-gap-coupled microstrip filter. $\epsilon_{r1} = 1.0$, $\epsilon_{r2} = 9.8$, $\epsilon_{r3} = 2.2$, $h_2 = h_3 = 0.01$, $l_1 = 0.2752$, $l_2 = 0.2542$, $l_3 = 0.2851$, $x_1 = 0.0516$, $x_2 = 0.0152$, $x_3 = 0.0106$. Unit of dimension: inch.

Fig. 5(a). Fed from port 2, the transversal dipole is excited at its resonant frequency of 9.6 GHz. The current is shown in Fig. 5(b). At 11.3 GHz, the coupling bend consisting of two perpendicular half-dipole is resonant. The incident power is essentially transmitted from one port to the other, and the current distribution is shown in Fig. 5(c). The magnitude of S-parameters is given in Fig. 5(d). The measured data are available from [33]. The good agreement can be observed. In this example, the number of unknowns is 912. The direct method takes 104 s for each frequency, and a total of 80 sampling frequencies are used to obtain the accurate results. Therefore, the total CPU time is approximately 139 min. In contrast, with AWE, only three expansion frequencies are needed. At each expansion point, the CPU time is 350.2 s. Totally, the CPU time is 17.5 min. Thus, using AWE is approximately eight times faster.

The final example is an overlap-gap-coupled microstrip filter [6], [34], illustrated in Fig. 6(a), which is a two-layer geometry. The top layer is alumina with a relative permittivity of 9.8 and a thickness of 0.254 mm. The bottom layer is duroid with a relative permittivity of 2.2 and a thickness of 0.254 mm. The geometrical parameters are the same as those in [34]. The number of unknowns is 503. In the direct calculation, the CPU time at each frequency is 27 s, and a total of 400 sampling frequencies are used to obtain the accurate results. Therefore, the total CPU time is approximately 3 h. The computed S-parameters in comparison with the measured data are shown in Fig. 6(b). The small discrepancy with the measured data is due to the finite thickness of metallization and the manufacturer's tolerance of substrates, as discussed in [6] and [34]. In contrast, with AWE, only nine expansion frequencies are chosen automatically by the binary search. At each expansion point, the CPU time is 95.9 s. In total, the CPU time is 863.1 s. Thus, the method with AWE is approximately 12.5 times faster than the direct calculation. The results without and with AWE are in excellent agreement, as shown in Fig. 6(c).

IV. Conclusion

This paper presents an efficient MoM solution of the MPIE formulation for a general microstrip structure in a multilayer

medium. In this method, the spectral-domain Green's functions for multilayer media are derived and the spatial-domain Green's functions in the form of SI's are then evaluated by the DCIM, which obviates the time-consuming numerical integration. The RWG basis functions are employed to provide necessary flexibility to model arbitrary shapes. The AWE is applied to efficiently evaluate the frequency response over a band of interest. Some multilayer circuits and antennas are analyzed to demonstrate the efficiency and accuracy of this method. We remark that since the sruface-wave contribution is not extracted, the error of the DCIM employed in this paper increases as the $k_0\rho$ increases. For all the examples, the error is within an acceptable tolerance for $k_0\rho < 100$ or $\rho < 16\lambda_0$, where λ_0 is the free-space wavelength. Most microstrip circuit components have a dimension much smaller than $16\lambda_0$, which is the primary reason for the accuracy of the proposed method.

REFERENCES

[1] K. C. Gupta and M. D. Abouzahra, Eds., *Analysis and Design of Planar Microwave Components*. Piscataway, NJ: IEEE Press, 1994.

[2] S. M. Rao, D. R. Wilton, and A. W. Glisson, "Electromagnetic scattering by surface of arbitrary shape," *IEEE Trans. Antennas Propagat.*, vol. AP-30, pp. 409–418, May 1982.

[3] K. L. Wu, J. Litva, R. Fralich, and C. Wu, "Full-wave analysis of arbitrarily shaped line-fed microstrip antennas using triangular finite-element method," *Proc. Inst. Elect. Eng.*, vol. 138, pt. H, pp. 421–428, Oct. 1991.

[4] K. A. Michalski and D. Zheng, "Analysis of microstrip resonators of arbitrary shape," *IEEE Trans. Microwave Theory Tech.*, vol. 40, pp. 112–119, Jan. 1992.

[5] R. A. Kipp and C. H. Chan, "Triangular-domain basis functions for full-wave analysis of microstrip discontinuities," *IEEE Trans. Microwave Theory Tech.*, vol. 41, pp. 1187–1194, June 1993.

[6] M. J. Tsai, F. D. Flaviis, O. Fordham, and N. G. Alexopoulos, "Modeling planar arbitrarily shaped microstrip elements in multilayered media," *IEEE Trans. Microwave Theory Tech.*, vol. 45, pp. 330–337, Mar. 1997.

[7] W. P. Harokopus and P. B. Katehi, "Characterization of microstrip discontinuities on multilayer dielectric substrates including radiation losses," *IEEE Trans. Microwave Theory Tech.*, vol. 37, pp. 2058–2066, Dec. 1989.

[8] W. Schwab and W. Menzel, "On the design of planar microwave components using multilayer structures," *IEEE Trans. Microwave Theory Tech.*, vol. 40, pp. 67–72, Jan. 1992.

[9] E. K. L. Yeung, J. C. Beal, and Y. M. M. Antar, "Multilayer microstrip structure analysis with matched load simulation," *IEEE Trans. Microwave Theory Tech.*, vol. 43, pp. 143–149, Jan. 1995.

[10] J. R. Mosig and F. E. Gardiol, "A dynamical radiation model for microstrip structures," in *Advances in Electronics and Electron Physics, Vol. 59*. New York, Academic, 1982, pp. 139–237.

[11] D. R. Jackson and N. G. Alexopoulos, "An asymptotic extraction technique for evaluating Sommerfeld-type integrals," *IEEE Trans. Antennas Propagat.*, vol. AP-34, pp. 1467–1470, Dec. 1986.

[12] D. C. Chang and J. X. Zhang, "Electromagnetic modeling of passive circuit elements in MMIC," *IEEE Trans. Microwave Theory Tech.*, vol. 40, pp. 1741–1747, Sept. 1992.

[13] D. G. Fang, J. J. Yang, and G. Y. Delisle, "Discrete image theory for horizontal electric dipole in a multilayer medium," *Proc. Inst. Elect. Eng.*, vol. 135, pt. H, pp. 297–303, Oct. 1988.

[14] Y. L. Chow, J. J. Yang, D. G. Fang, and G. E. Howard, "A closed-form spatial Green's function for the thick microstrip substrate," *IEEE Trans. Microwave Theory Tech.*, vol. 39, pp. 588–592, Mar. 1991.

[15] R. A. Kipp and C. H. Chan, "Complex image method for sources in bounded regions of multilayer structures," *IEEE Trans. Microwave Theory Tech.*, vol. 42, pp. 860–865, May 1994.

[16] G. Dural and M. I. Aksun, "Closed-form Green's functions for general sources and stratified media," *IEEE Trans. Microwave Theory Tech.*, vol. 43, pp. 1545–1552, July 1995.

[17] M. I. Aksun, "A robust approach for the derivation of closed-form Green's functions," *IEEE Trans. Microwave Theory Tech.*, vol. 44, pp. 651–658, May 1996.

[18] Y. Hua and T. K. Sarkar, "Generalized pencil-of-function method for extracting poles of an EM system from its transient response," *IEEE Trans. Antennas Propagat.*, vol. 37, pp. 229–234, Feb. 1989.

[19] W. C. Chew, *Waves and Fields in Inhomogeneous Media*. Piscataway, NJ: IEEE Press, 1995.

[20] K. A. Michalski and J. R. Mosig, "Multilayered media Green's functions in integral equation formulations," *IEEE Trans. Antennas Propagat.*, vol. 45, pp. 508–519, Mar. 1997.

[21] Y. L. Chow, N. Hojjat, S. Safavi-Naeini, and R. Faraji-Dana, "Spectral Green's functions for multilayer media in a convenient computational form," *Proc. Inst. Elect. Eng.*, vol. 145, pt. H, pp. 85–91, Feb. 1998.

[22] L. T. Pillage and R. A. Rohrer, "Asymptotic waveform evaluation for timing analysis," *IEEE Trans. Computer-Aided Design*, vol. 9, pp. 352–366, Apr. 1990.

[23] E. Chiprout and M. S. Nakhla, "Analysis of interconnect networks using complex frequency hopping," *IEEE Trans. Computer-Aided Design*, vol. 14, pp. 186–200, Feb. 1995.

[24] P. Feldmann and R. W. Freund, "Efficient linear circuit analysis by Padé approximation via the Lanczos process," *IEEE Trans. Computer-Aided Design*, vol. 14, pp. 639–649, May 1995.

[25] M. A. Kolbehdari, M. Srinivasan, M. S. Nakhla, Q. J. Zhang, and R. Achar, "Simultaneous time and frequency domain solutions of EM problems using finite element and CFH techniques," *IEEE Trans. Microwave Theory Tech.*, vol. 44, pp. 1526–1534, Sept. 1996.

[26] J. P. Zhang and J. M. Jin, "Preliminary study of AWE method for FEM analysis of scattering problems," *Microwave Opt. Technol. Lett.*, vol. 17, pp. 7–12, Jan. 1998.

[27] C. J. Reddy, M. D. Deshpande, C. R. Cockrell, and F. B. Beck, "Fast RCS computation over a frequency band using method of moments in conjunction with asymptotic waveform evaluation technique," *IEEE Trans. Antennas Propagat.*, vol. 46, pp. 1229–1233, Aug. 1998.

[28] J. E. Bracken, D. K. Sun, and Z. J. Cendes, "S-domain methods for simultaneous time and frequency characterization of electromagnetic devices," *IEEE Trans. Microwave Theory Tech.*, vol. 46, pp. 1277–1290, Sept. 1998.

[29] G. J. Burke, E. K. Miller, S. Chakrabarthi, and K. Demarest, "Using model-based parameter estimation to increase the efficiency of computing electromagnetic transfer functions," *IEEE Trans. Magn.*, vol. 25, pp. 2807–2809, July 1989.

[30] J. E. Pekarek and T. Itoh, "Use of frequency derivatives in the three-dimensional full-wave spectral-domain technique," *IEEE Trans. Microwave Theory Tech.*, vol. 44, pp. 2466–2472, Dec. 1996.

[31] M. Davidovitz and Y. T. Lo, "Rigorous analysis of a circular patch antenna excited by a microstrip transmission line," *IEEE Trans. Antennas Propagat.*, vol. 37, pp. 949–958, Aug. 1989.

[32] D. I. Wu, D. C. Chang, and B. L. Brim, "Accurate numerical modeling of microstrip junctions and discontinuities," *Int. J. Microwave Millimeter-Wave Computer-Aided Eng.*, vol. 1, pp. 48–58, Jan. 1991.

[33] R. Gillard, J. Corre, M. Drissi, and J. Citerne, "A general treatment of matched terminations using integral equations—Modeling and application," *IEEE Trans. Microwave Theory Tech.*, vol. 42, pp. 2545–2553, Dec. 1994.

[34] O. Fordham, M. J. Tsai, and N. G. Alexopoulos, "Electromagnetic synthesis of overlap-gap-coupled microstrip filters," in *IEEE MTT-S Int. Microwave Symp. Dig.*, 1995, pp. 1199–1202.

Feng Ling (S'97) was born in Jiangsu, China, in 1971. He received the B.S. and M.S. degrees in electrical engineering from Nanjing University of Science and Technology, Nanjing, China, in 1993 and 1996, respectively, and is currently working toward the Ph.D. degree in electrical engineering at the University of Illinois at Urbana-Champaign.

Since 1996, he has been a Research Assistant at the Center for Computational Electromagnetics, University of Illinois at Urbana-Champaign. His research interests include electromagnetic modeling of microwave integrated circuits and microstrip antennas, and fast algorithms for computational electromagnetics.

Mr. Ling is a member of Phi Kappa Phi. He was the recipient of the 1999 Y. T. Lo Outstanding Research Award presented by the Department of Electrical and Computer Engineering, University of Illinois at Urbana-Champaign.

Dan Jiao was born in Anhui Province, China, in 1972. She received the B.S. and M.S. degrees in electrical engineering from Anhui University, Anhui, China, in 1993 and 1996, respectively, and is currently working toward the Ph.D. degree in electrical engineering at the University of Illinois at Urbana-Champaign.

From 1996 to 1998, she performed graduate duties at the University of Science and Technology of China, Hefei, China. Since 1998, she has been a Research Assistant at the Center for Computational Electromagnetics, University of Illinois at Urbana-Champaign. Her current research interests include fast computational methods in electromagnetics.

Jian-Ming Jin (S'87–M'89–SM'94) received the B.S. and M.S. degrees in applied physics from Nanjing University, Nanjing, China, in 1982 and 1984, respectively, and the Ph.D. degree in electrical engineering from The University of Michigan at Ann Arbor, in 1989.

He is an Associate Professor of Electrical and Computer Engineering and Associate Director of the Center for Computational Electromagnetics at the University of Illinois at Urbana-Champaign. He has authored or co-authored over 70 papers in refereed journals and several book chapters. He has also authored *The Finite Element Method in Electromagnetics* (New York: Wiley, 1993) and *Electromagnetic Analysis and Design in Magnetic Resonance Imaging* (Boca Raton, FL: CRC Press, 1998) and co-authored *Computation of Special Functions* (New York: Wiley, 1996). His current research interests include computational electromagnetics, scattering and antenna analysis, electromagnetic compatibility, and magnetic resonance imaging. His name is listed in the University of Illinois at Urbana-Champaign's *List of Excellent Instructors*. He currently serves as an associate editor of *Radio Science* and is also on the Editorial Board for the *Electromagnetics Journal* and *Microwave and Optical Technology Letters*.

Dr. Jin is a member of Commission B of USNC/URSI, Tau Beta Pi, and the International Society for Magnetic Resonance in Medicine. He was a recipient of the 1994 National Science Foundation Young Investigator Award and the 1995 Office of Naval Research Young Investigator Award. He also received the 1997 Xerox Research Award presented by the College of Engineering, University of Illinois at Urbana-Champaign, and was appointed as the first Henry Magnuski Outstanding Young Scholar in the Department of Electrical and Computer Engineering in 1998. He served as an associate editor for the IEEE TRANSACTIONS ON ANTENNAS AND PROPAGATION (1996–1998). He was the symposium co-chairman and technical program chairman of the International Symposia on Applied Computational Electromagnetics in 1997 and 1998, respectively.